Activation/Deactivation Free-Energy Profiles for the β_2-Adrenergic Receptor: Ligand Modes of Action

Jacqueline C. Calderón,[a] Passainte Ibrahim,[b] Dorothea Gobbo,[c,d] Francesco Luigi Gervasio[c,d,e,f] and Timothy Clark.[a]

[a] Computer-Chemistry-Center, Department of Chemistry and Pharmacy, Friedrich-Alexander-University Erlangen-Nuernberg, Naegelsbachstr. 25, 91052 Erlangen, Germany.

[b] Institute of Medical Physics and Biophysics, Faculty of Medicine, University of Leipzig, Germany.

[c] Pharmaceutical Sciences, University of Geneva, CH1206, Geneva, Switzerland.

[d] Institute of Pharmaceutical Sciences of Western Switzerland, CH1206 Geneva, Switzerland.

[e] Chemistry Department, University College London, WC1H 0AJ London, UK.

[f] Swiss Bioinformatics Institute, CH1206, Geneva, Switzerland.

* Timothy Clark & Francesco Luigi Gervasio.

Email: Tim.Clark@fau.de; Francesco.Gervasio@unige.ch

G protein coupled receptor, beta-adrenergic receptor, receptor activation, partial agonism, metadynamics

ABSTRACT

We use enhanced-sampling simulations with an effective collective variable to study the activation of the β_2-adrenergic receptor in the presence of ligands with different efficacy. The free-energy profiles are computed for the ligand-free (*apo*) receptor and binary (*apo*-receptor + G protein α-subunit and receptor + ligand) and ternary complexes. The results are not only compatible with available experiments but also allow unprecedented structural insight into the nature of GPCR conformations along the activation pathway and their role in the activation mechanism. In particular, the simulations reveal an unexpected mode of action of partial agonists such as salmeterol and salbutamol that arises already in the binary complex without the G-protein. Specific differences in the polar interactions with residues in TM5, which are required to stabilize an optimal TM6 conformation facilitating G-protein binding and receptor activation, play a major role in differentiating them from full agonists.

INTRODUCTION

G protein coupled receptors (GPCRs) are the most important class of signaling receptors in mammalian genomes, with more than 800 occurring in humans.[1] Consequently, up to half of all marketed drugs target GPCRs. Except for rhodopsin, the prototypical β_2-adrenergic receptor (ADRB2) is perhaps the most extensively characterized member of the GPCR family, for which a wealth of experimental and computational data and ligands of different types is available.[2,3,4,5,6,7,8,9,10,11,12,13,14,1516,17] GPCR ligands are typically categorized as full agonist, partial agonist, neutral antagonist, and inverse agonists according to their capability to elicit the maximum response for specific signaling pathways. Antagonists of the adrenergic receptor, more commonly known as β-blockers, are widely used in clinical practice, but they are also linked to undesirable side-effects.[18] Therefore, partial agonists have emerged as a viable alternative whenever overstimulation of a GPCR needs to be prevented by tuning the receptor response.[19] Despite the efforts made to gain insights into the partial agonism at adrenergic receptors[4,5,9,14,20] the structural mechanisms driving ligand efficacy and GPCRs activation are not fully understood.

Because GPCRs dynamics is experimentally challenging,[21] molecular dynamics (MD) simulations[2,3,4,22,23,24,25,26,27] and enhanced sampling algorithms,[28] such as string method[4,5] and complex multi-collective variable metadynamics simulations[29] have played a major part in revealing details of the activation process of GPCRs. Recently, we have proven it possible to define a generally applicable single collective variable (CV) not only for ligand binding/unbinding[30] but also for activation/deactivation[31] in class A GPCRs.

Here we apply our standard activation/deactivation metadynamics-based protocol[31] to characterize the free-energy landscape underlying the activation mechanism of ADRB2 in complex with full agonists (adrenaline,[32] BI167107,[7] isoprenaline,[33] and formoterol[34]), partial agonists (salmeterol[9] and salbutamol[33]), antagonists (alprenolol[35], carvedilol[36] and propranolol[36]), and inverse agonists (carazolol[37], ICI118,551[35], and timolol[36]). By re-projecting the free-energy profiles on a selection of microswitches defined previously,[2,4,38] we were able to provide a detailed structural characterization of ADRB2 conformations accessible during activation suggesting correlations between receptor conformation and ligand efficacy. Of particular value for validating our results are recent NMR investigations,[15,16,39] which characterize the transition from a pre-active conformation formed in binary receptor-ligand complexes to a fully active one upon binding of a G protein.

RESULTS AND DISCUSSION

Activation/deactivation free-energy profiles

Multiple-walker metadynamics simulations were performed using the A^{100} index[40] as CV. A^{100} is a linear combination of five inter-helix (C_α-C_α) distances that was trained using simulation data to characterize the activation state of class A GPCRs. It was validated with all the then available X-ray crystal structures using the activation states defined by the experimentalists. A^{100} was originally defined using a three-state (active, intermediate, and inactive) model, but a two state (active, inactive) model using A^{100}=25 as the border between states ($A^{100} \geq 25$ = active) was found to be more reliable and is used in this work.

The use of multiple-walker metadynamics simulations[41] is important. Using A^{100} as a single activation CV represents a drastic reduction in dimensionality, which might result in incomplete

sampling using standard metadynamics. Because each independent walker contributes to the total potential, multi-walker metadynamics drastically improves the sampling.[41] By choosing walkers that are initially well distributed along the CV and by monitoring crossing events between CV windows carefully, very effective sampling of the degrees of freedom not represented by the CV can be obtained. Furthermore, as observed when developing A^{100},[40] the activity of the receptor conformation can be represented by a large number of strongly correlated linear combinations of interatomic distances, so that any one of these linear combinations is likely to include the relevant slow degrees of freedom. This "delocalized" representation of receptor activation implicitly includes many slow degrees of freedom that are sometimes indicative of activation. In some respects, A^{100} functions analogously to a principal component. Combined with well-tempered metadynamics, this delocalized nature of the CV guarantees convergence of the simulations with adequate sampling.[42]

It is clear that A^{100} represents a very significant dimensionality reduction when used as an activation/deactivation CV. In our original paper on the use of A^{100} for this purpose,[31] we therefore defined very stringent quality checks to ensure that the simulations reproduce as many subtle conformational changes as possible. A major tool in this respect is to re-project the simulation results onto the so-called microswitches, conserved interactions that have been suggested to be characteristic of active or inactive conformations.[31] We have followed the same methodology here, so that we consider our results to be meaningful.

Additionally, we have analyzed the metadynamics simulation for the *apo*-ADRB2 receptor in terms of the root mean square deviations (RMSD) of all structures within five A^{100} units of the minimum. These histograms (Figure S1 in the Supporting Information) show single conformations with a peak at RMSD = 0.26 nm for the global minimum and 0.25 nm for the secondary minimum.

The latter shows 12 structures with RMSD > 0.27 nm on the high side of the major distribution peak.

The resulting free-energy profiles of the receptor in its *apo* state and bound to ligands with different efficacies and the α-subunit of the Gs protein ($G_{\alpha s}$) are shown in Figures 1 and 2. For each system, we assess the correlation between the mean A^{100}-value over the last 500 ns of 2 μs unconstrained simulations and the deepest minimum found in the metadynamics simulations to check the consistency between the most populated conformations sampled in plain MD and enhanced sampling (Figure S2). To ensure a balance of computational cost and accuracy, convergence of the metadynamics simulations is verified by monitoring:

a. time-dependent evolution of the calculated free-energy profile as a function of A^{100},

b. time-dependent evolution of the Gaussian hills height deposited during the A^{100} metadynamics simulations,

c. comparison between the free-energy values as a function of the A^{100} obtained from the metadynamics bias potential and by reweighting,

d. the calculated error in the reconstructed free energy profiles and,

e. activation/deactivation CV as a function of the sampling time for 32 walkers.

To further demonstrate the reliability of the metadynamics protocol, three independent replicas of the ADRB2-isoprenaline complex were run. As expected, only small differences among the three free energy profiles can be observed (Figure S3): These can be attributed to the initial random velocities.

Figures S4-6 show the plots used to determine the convergence of the multiple-walker metadynamics simulations for three replicas of the ADRB2-isoprenaline complex. As can be observed from Figures S4A, S5A, and S6A, the estimated free energy does not change significantly as a function of time for the last 500 ns of the simulation. It is evident from Figures S4B, S5B, and S6B that the Gaussian hills height decreases to values lower than 0.05 kcal.mol^{-1} for the three simulations. While only slight differences can be observed when comparing the A^{100} free-energy profile calculated from the metadynamics bias potential with the one obtained through the reweighting procedure (Figures S4C, S5C, and S6C). The average error of the MW-metadynamics simulations was obtained though block analysis (details in the SI). As expected, the error increases with the block size until it reaches a plateau with a value of ~0.3 kcal.mol^{-1} for the three simulations (Figures S4D, S5D, and S6D). In addition, sampling of the conformational space was tracked by inspecting the individual trajectories for each walker. Figures S4E, S5E, and S6E show that walkers frequently and reversibly visit neighboring regions of the CV space. The convergence behavior of criteria *a, b*, *c,* and *d* for the other ADRB2 systems is similar, as can be seen from Figures S7-10.

In addition, sampling of the CV space is not only enhanced for the A^{100} index, but also for the set of microswitches, which were not directly biased during the metadynamics simulations (Figures S11-14).

Systems	A^{100} MD	A^{100} MetaD
ADRB2	18.4	20.4
ADRB2-$G_{\alpha s}$	40.4	40.4
ADRB2-adrenaline	-5.2	19.6
ADRB2-adrenaline-$G_{\alpha s}$	34.6	38.9
ADRB2-BI167107	-30.6	-42.0
ADRB2-BI167107-$G_{\alpha s}$	36.2	30.2
ADRB2-isoprenaline	4.2	-2.2
ADRB2-isoprenaline-$G_{\alpha s}$	54.5	28.6
ADRB2-formoterol	11.3	10.4
ADRB2-formoterol-$G_{\alpha s}$	43.1	41.9

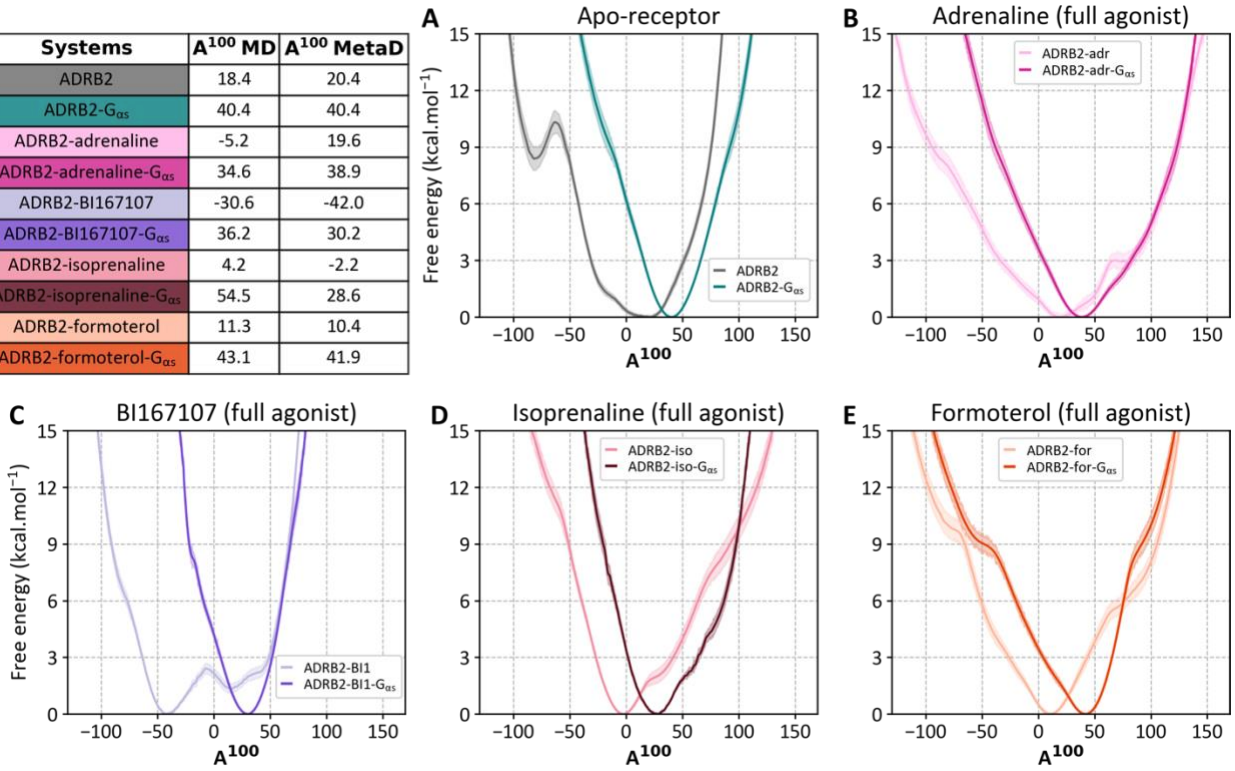

Figure 1. Simulation results for *apo*-ADRB2 and agonist-bound ADRB2 systems. Calculated activation/deactivation free-energy profiles from MW metadynamics simulations. Shaded error bands show the estimates of uncertainty in the free-energy profiles. The mean A^{100}-values for the last 500 ns of the unbiased simulations and the A^{100} values corresponding to the lowest minima in the free-energy curves are also reported. For orientation, in the two-state model,[40] $A^{100} > 25$ and $A^{100} < 25$ indicate activation and deactivation, respectively.

In the absence of an activating ligand GPCRs normally exhibit basal (constitutive) activity. Basal activity has been explained by small energy differences between the inactive and active states and a lower energy barrier that would increase the probability of spontaneous conformational transitions to the active state.[21,43,44,45,46,47] However, these explanations may be too simplistic. Our results suggest that the ability of the *apo*-receptor to recruit the G-protein may be the key step in determining basal activity. When compared with Figures 1B-E, Figure 1A suggests that, once it has recruited a G-protein, the *apo*-receptor is very similar to that bound to a full agonist. The difference therefore likely lies in the ability of the *apo*-receptor or the agonist:receptor binary complex to recruit the G-protein. This latter process is not covered by A^{100} and therefore not reflected in our current results. We note, however, that it is possible to determine G-protein binding

energies using metadynamics.[48] Developing a standard protocol for these calculations is necessary in order to obtain a complete picture of GPCR activation.

Experiments show that the binding of a full or partial agonist to a ligand-free GPCR increases the frequency of activation transitions, while reducing the frequency of deactivating events, probably lowering the energy barrier and/or reducing the energy of the more active conformation relative to the inactive conformation. In contrast, inverse agonist binding increases the frequency of deactivation transitions, thus increasing the energy barrier and/or reducing the energy of the inactive state conformation relative to the active conformation.[46,47]

Figure 1A shows the activation/deactivation free-energy profiles of both *apo*-ADRB2 and *apo*-ADRB2-$G_{\alpha s}$. The receptor without the G-protein shows a broad global minimum at A^{100}-values between 0 and 26, suggesting the presence of either several isoenergetic conformations mostly belonging to the inactive-like state or a single very flexible inactive-like state. Note that we use the two-state A^{100} model ($A^{100} \geq 25$ = active)[40] throughout this work. This observation suggests that *apo*-ADRB2 mostly adopts an inactive conformation and is able to fluctuate spontaneously between inactive and active-like conformations, in agreement with the experimentally observed high basal activity for the ADRB2.[46,47] In contrast, the free-energy profile for the *apo*-ADRB2-$G_{\alpha s}$ binary complex shows one narrow minimum in the active region at $A^{100} = 40.4$. The effect of the G-protein on the conformational flexibility of *apo*-ADRB2 is evident, not only does it shift the minimum to a more active A^{100}-value, but it also limits ADRB2 structural flexibility, consistently to the experimentally observed stabilization of the β_1-adrenergic receptor (ADRB1) upon coupling to an intracellular binding partner (IBP).[39] As previously suggested,[31] A^{100} alone does not allow to clearly discriminate conformations belonging to energetically similar free-energy minima, thus

requiring the re-projection of the free-energy profiles along different reaction coordinates (see below).

The results for the *apo*-ADRB2 agree not only with the accepted notion that the ligand-free ADRB2 is structurally dynamic[21,43,44,45,46,49,50] and exists in an ensemble of basal conformational states, but also with the possibility of one predominantly constrained state with a relatively high affinity for IBPs.[43]

Agonist ligand complexes

Figures 1B-E show the free-energy landscapes for ADRB2 complexes with the full agonist ligands adrenaline,[32] BI167107,[7] isoprenaline,[33] and formoterol.[34] The free-energy simulations for the binary complex with the natural ligand adrenaline (Figure 1B) result in a global minimum at A^{100} = 19.6, with a 3 kcal mol^{-1} less stable shoulder at $A^{100} \approx 67$ in the active region, which may indicate a metastable active-like conformation. The ternary ADRB2-adrenaline-$G_{\alpha s}$ complex exhibits a steep global minimum for an active conformation at A^{100} = 38.9. The binary complex of the receptor with the strong agonist BI167107 (ADRB2-BI167107) (Figure 1C) shows two minima within the inactive region of the two-state model[40] (A^{100} = -42.0 and 15.8) and a third less stable one (+1.9 kcal mol^{-1}) in the active region (A^{100} = 40.4). In contrast, the ternary ADRB2-BI167107-$G_{\alpha s}$ complex shows only the fully activated minimum at A^{100} = 30.2, indicating a relatively inflexible active conformation. The free energy profiles for ADRB2 with bound isoprenaline and formoterol agonists are comparable (Figures 1D and 1E, respectively) since each exhibits a free-energy minimum for the inactive conformation (A^{100} = -2.2 and 10.4, respectively) and a hint of a shoulder at active A^{100}-values. Analogously to previous cases reported here, ternary complexes

with isoprenaline and formoterol show steep minima in the active region at A^{100}-values of 28.6 and 41.9, respectively.

NMR studies[39] demonstrate that full agonists binding to the β_1-adrenergic receptor results in a highly dynamic pre-activated receptor form sampling multiple active-like conformations competent to bind IBPs, with adrenaline-bound ADRB1 appearing more dynamic than isoprenaline binary complex and ADRB1 in the *apo* form. In agreement with NMR data, the broad global minimum found in the free-energy profile for ADRB2-adrenaline binary complex suggests the presence of multiple iso-energetic conformations or a single very flexible state, in the same way as in the *apo*-ADRB2, with a clear shift towards the A^{100} active region. Differently, for ADRB2-isoprenaline, the sharper global minimum hints a relatively inflexible receptor bound state. As described below, by re-projecting the 1D free-energy profiles on different reaction coordinates and comparing the most stable A^{100} free-energy basin, we were able to identify the relevant structural features establishing the different flexibility patterns observed for agonist-bound ADRB2.

The results of the metadynamics simulations for ADRB2 complexes with the partial agonists salmeterol[9] and salbutamol[33] are shown in Figures 2B and 2C, respectively. In both ternary complexes, the deepest free-energy minima are well within the active region of the two-state model,[40] with A^{100} equal to 57.4 for ADRB2-salmeterol-$G_{\alpha s}$ and 36.6-58.0 for ADRB2-salbutamol-$G_{\alpha s}$. Activation/deactivation curves for salmeterol- and salbutamol-bound ADRB2 show one global minimum in the inactive region (A^{100} equal to 21.1 for ADRB2-salmeterol and 23.2 for ADRB2-salbutamol) and a secondary minimum in the active one at A^{100} = 84.7 ($\Delta\Delta G$ = 6.2 kcal mol^{-1}) and A^{100} = 93-128 ($\Delta\Delta G$ = 10.2 kcal mol^{-1}) for ADRB2-salmeterol and ADRB2-salbutamol, respectively.

It is noteworthy that the free-energy profiles for binary complexes with partial agonist salmeterol (Figure 2A) and full agonist formoterol (Figure 1E) show a secondary minimum in the active A^{100} region approximately 6.0 kcal mol^{-1} higher in energy. Formoterol is a full agonist that can also be classified as a partial agonist of high intrinsic efficacy, whereas salmeterol is a partial agonist of low intrinsic efficacy. The similarity between the computed free-energy landscapes might thus reflect the similar pharmacological profiles of these clinically interchangeable compounds.[51,52,53] The free-energy profiles computed for ADRB2 in complex with full and partial agonists are consistent with the experimentally observed preference of the agonist-bound receptor for the inactive conformation. In absence of a stabilizing interaction with a G protein or nanobody, adrenergic receptors with bound agonists have been solved in inactive conformations only.[54,55,56] In addition, both previous molecular dynamics studies[2,54] and results reported here (Figures S15-19), suggest that an agonist-bound active conformation spontaneously relaxes to an inactive-like conformation in the absence of stabilizing IBP.

Antagonist and inverse agonist ligand complexes

Figure 2C shows the results of the metadynamics simulations for binary ADRB2 complexes with the antagonists alprenolol,[35] carvedilol[36] and propranolol.[36] Alprenolol shows a minimum at A^{100} = -12.2 and a shoulder in the weakly active region at $A^{100} \approx 26$. The free-energy profile for propranolol displays one broad global minimum spanning A^{100}-values between 0 and 26. Thus, both alprenolol and propranolol give the expected free-energy profiles for neutral antagonists, which have no effect on basal activity but competitively block access of other ligands. The free-energy profile for carvedilol displays a clear secondary minimum in the inactive region approximately 8.5 kcal mol^{-1} higher in energy similar to the one identified for *apo*-ADRB2, but

this minimum is too high in energy to be relevant under physiological conditions. The deepest minimum at $A^{100} = 1.2$ spreads to the inactive region with little increase in energy while an unstable shoulder in the active region can be found at $A^{100} = 50$, similar to the one observed for alprenolol binary complex.

Systems	A^{100} MD	A^{100} MetaD
ADRB2-salmeterol	10.9	21.1
ADRB2-salmeterol-$G_{\alpha s}$	42.5	57.4
ADRB2-salbutamol	17.9	23.2
ADRB2-salbutamol-$G_{\alpha s}$	42.9	40.3
ADRB2-alprenolol	-14.8	-12.2
ADRB2-carvedilol	0.2	1.9
ADRB2-propranolol	6.4	6.0
ADRB2-carazolol	-23.6	-28.7
ADRB2-ICI118,551	-23.0	-31.6
ADRB2-timolol	-9.7	-3.3

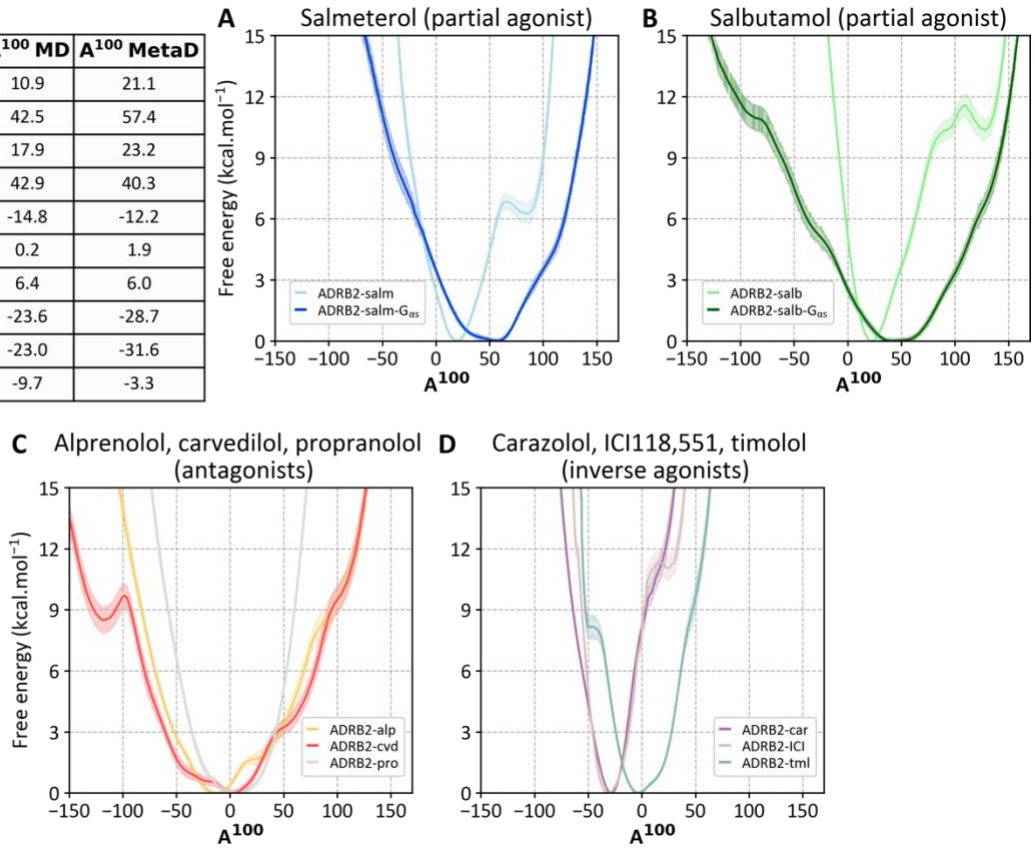

Figure 2. Simulation results for ADRB2 systems in complex with partial agonist, antagonist, and inverse agonist ligands. Calculated activation/deactivation free-energy profiles from MW metadynamics simulations. Shaded error bands show the estimates of uncertainty in the free-energy profiles. The mean A^{100}-values for the last 500 ns of the unbiased simulations and A^{100} values corresponding to the lowest minima in the free-energy curves are also reported. For orientation, in the two-state model,[40] $A^{100} > 25$ and $A^{100} < 25$ indicate activation and deactivation, respectively.

Figure 2D shows the free-energy profiles obtained for binary ADRB2 complexes with the inverse agonists carazolol,[37] ICI118,551,[35] and timolol.[36] As expected, all three inverse agonists give the deepest minima well into the inactive range (A^{100} equal to -28.7, -31.6 and -3.3 for carazolol, ICI118,551 and timolol, respectively). The profile for ICI118,551 shows a secondary minimum

around A^{100} = 23 and a shoulder for timolol is found at A^{100} =- 45, again in the inactive A^{100}-range of values in the two-state model.[40] These results are consistent with the well-known inverse-agonist activity profiles of these three ligands.

Structural determinants of ligand activity

In the following discussion, we assume that, as found experimentally[15,39] and also computationally for a class B GPCR,[29] a pre-active conformation is accessible in the binary receptor-agonist complex and a fully active one in the ternary complex with an IBP. As stated previously[31] and found here (Figures S20-23), the A^{100} index does not map uniquely to individual structures, thus is not able to distinguish between pre-active and fully active conformations. Therefore, to capture the complexity of the conformational fluctuations of the receptor in complex with ligands with different efficacy, we reweighted our A^{100} metadynamics simulations to reconstruct 1D and 2D free-energy landscapes along a set of conserved microswitches identified previously[2,4,38] (Details in Table S1).

The 1D free-energy landscapes projected as a function of the microswitches for the *apo*-receptor and ADRB2-ligand systems are shown in Figure 3. The first important conclusion is that for the *apo*-receptor the TM3-TM6 distance can explore values ranging between 0.70 and 1.50 nm essentially without energetic penalty (+1 kcal mol^{-1}). The same is true for the YY distance (0.58-1.21 nm) and the NPxxY (0.26-0.45 nm) and PIF (0.13-0.42 nm) RMSDs. Thus, as might be expected, the microswitches for the *apo*-receptor in the absence of a G-protein are agnostic to the activation state of the receptor, in contrast to A^{100} (Figure 1A), highlighting the flexibility of the *apo*-ADRB2 and its preference for the inactive state.

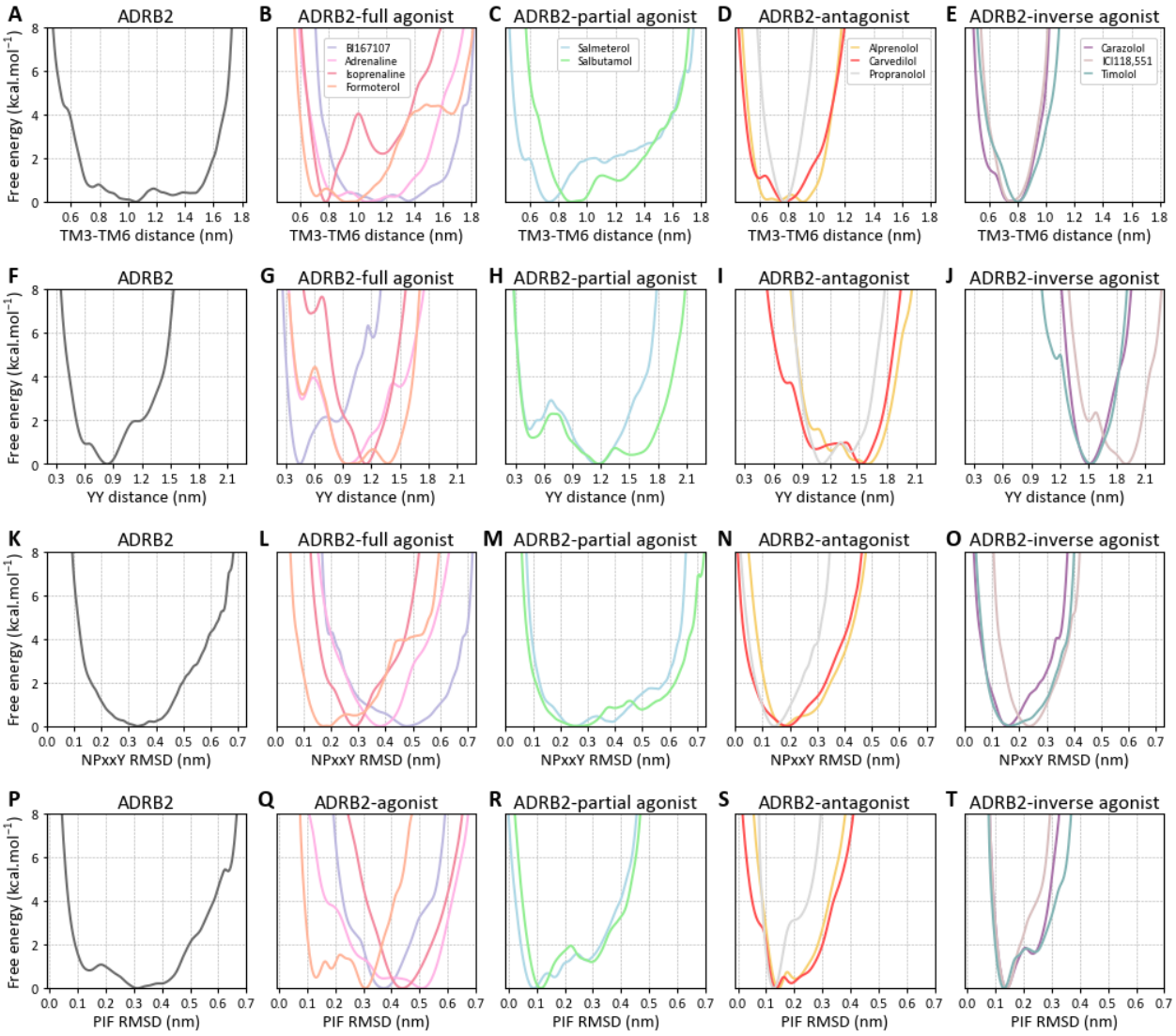

State of the microswitches

Systems	TM3-TM6 distance	YY distance	NPxxY RMSD	PIF RMSD
ADRB2	intermediate	intermediate	intermediate	intermediate
ADRB2-adrenaline	intermediate	intermediate	active	active
ADRB2-BI167107	intermediate	active	active	active
ADRB2-isoprenaline	inactive	intermediate	intermediate	active
ADRB2-formoterol	inactive	intermediate	inactive	intermediate
ADRB2-salmeterol	inactive	intermediate	intermediate	inactive
ADRB2-salbutamol	inactive	intermediate	intermediate	inactive
ADRB2-alprenolol	inactive	inactive	inactive	inactive
ADRB2-carvedilol	inactive	inactive	inactive	inactive
ADRB2-propranolol	inactive	intermediate	inactive	inactive
ADRB2-carazolol	inactive	inactive	inactive	inactive
ADRB2-ICI118,551	inactive	inactive	intermediate	inactive
ADRB2-timolol	inactive	inactive	inactive	inactive

Figure 3. Comparison of the free-energy landscapes projected as a function of the microswitches for all ADRB2 binary complexes. The state of each microswitch for all binary ADRB2 complexes relative to the global minima is specified in the table. Thresholds used to define active/intermediate/inactive states: TM3-TM6 distance ≥ 1.20 nm, 1.19-1.06 nm, ≤ 1.05 nm; YY distance ≤ 0.80 nm, 0.81-1.45 nm, ≥ 1.46 nm; NPxxY RMSD ≥ 0.34 nm, 0.33-0.21 nm, ≤ 0.20 nm; PIF RMSD ≥ 0.31 nm, 0.30-0.23 nm, ≤ 0.22 nm.

Significant differences can be observed for ADRB2-full agonist binary complexes. The uniquely strong agonist BI167107 behaves differently to the other full agonists as the global free-energy minimum indicates the most stable conformation adopting an intermediate-like state for the intracellular side of TM6 and active-like state for the YY distance, NPxxY and motifs (Figure 3B, G, L and Q respectively). TM3-TM6 free-energy profiles for BI167107, adrenaline and formoterol complexes suggest a flexible intracellular part of ADRB2, with formoterol shifting the equilibrium towards inactive TM3-TM6 distances. Differently, isoprenaline allows ADRB2 to access mainly inactive TM3-TM6 distances given the presence of a free-energy energy barrier of ~4 kcal mol^{-1} between the global and secondary minima. The water-mediated hydrogen bond between the two tyrosines subtends TM6 and is believed to stabilize its active conformation.[15] It is therefore not surprising that ADRB2 bound to BI167107, a highly potent agonist used to support the crystallization of active ADRB2 and ADRB2-G_s complexes,[7] shows a YY distance compatible with an active-like conformation. The YY-interaction is clearly broken in all the other ADRB2-full agonist systems, with global minima at YY distances spanning from 0.95 nm to 1.38 nm. Interestingly, adrenaline and formoterol result in similar free-energy profiles except for the double binned global minimum of formoterol which suggests a greater structural flexibility of the receptor at the intracellular side. Both ligands give access to active YY distances with little (< 4 kcal mol^{-1}) energy penalty. In contrast, isoprenaline seems unable to induce ADRB2 to adopt active-like YY distances in the absence of IBP. Consistently, free-energy profiles as a function of NPxxY RMSD indicate BI167107 as the most potent agonist of the series in shifting the equilibrium towards active-like NPxxY conformations followed by adrenaline, isoprenaline, and formoterol. Finally, PIF RMSD showcases adrenaline as the most effective agonist ligand in this series in shifting the receptor conformation in the transmembrane region towards the active state. The

sharper free-energy minima identified for BI1671097 and isoprenaline suggest a reduced flexibility of the most stable conformation in the PIF region, which still adopts active conformations. Differently, formoterol seems to be the only full agonist in the series to shift the equilibrium for the PIF motif towards intermediate-like conformations. The high structural variability detected for all the full agonist-bound ADRB2 systems strongly agrees with recent NMR studies[39] showing the increased structural flexibility of ADRB1-agonist binary complexes with respect to the *apo* state.

Unlike full agonists, partial agonist binary complexes show global minima located at more inactive regions of the TM3-TM6 distance (0.74-0.90 nm), YY distance (1.16-1.19 nm), NPxxY (0.26-0.28 nm) and PIF (0.09-0.12 nm) motifs. In line with previous observations, similarities between the free-energy profiles for partial agonists and formoterol can be detected, especially when comparing the TM3-TM6 distance and NPxxY RMSD relative position of the global minima (Figures 3B, C, L and M, respectively). In contrast to full agonists, in absence of IBP partial agonists seem unable to shift the conformational equilibrium of the PIF motif towards active-like states.

As expected, antagonists and inverse agonist binary complexes show, in general, global minima compatible with inactive-like states for all microswitches (TM3-TM6 (0.75-0.91 nm), YY (1.11-1.90 nm), NPxxY (0.14-0.24 nm) and PIF motifs (0.13-0.14 nm)), see Figure 3 state of the microswitches). Interestingly, partial agonist 1D free-energy profiles resemble those obtained for the antagonist-like ligands. This is noticeable for the PIF motif, for which a different pattern can be observed between full and partial agonist ligands (Figures 3Q and R). These results are not only consistent with the notion that ligands can stabilize different receptor states[57] but also suggest that,

in general, binding of a full agonist reduces the number of inactive-like states of the conserved microswitches in comparison to a partial agonist (Figure 3).

2D free-energy landscapes were defined by projecting the TM3-TM6 distance onto the YY distance, NPxxY and PIF motifs (Figures S24-26). For the *apo*-receptor and agonist bound-ADRB2 binary complexes, several clear minima can be seen that span regions compatible with active-, intermediate- and inactive-like states of the TM3-TM6 distance, YY distance, NPxxY and PIF motifs. In contrast, the TM3-TM6 distance is only populated at inactive-like conformations for antagonist and inverse agonist binary complexes as a result of the more rigid inactive-like conformations induced by ligands inhibiting ADRB2 activation. Interestingly, both inactive- and intermediate-like conformations of the YY distance, NPxxY and PIF motifs can be observed for the alprenolol complex even if TM3-TM6 distances show an inactive-like conformation.

The role the PIF motif plays in GPCR activation has been emphasized for different sub-families of GPCRs. Imai and coworkers[16] noticed that the configuration of the PIF motif in ADRB2 bound to partial agonists is close to that observed in the inactivated conformation. In a similar study by Eddy et al.,[58] NMR spectroscopy of partial agonist complexes of the A2A adenosine receptor revealed that, in the absence of interactions with IBPs, the conformation of the PIF motif is distinctly different from full agonist complexes. The mechanism in which agonists trigger the PIF motif rearrangement varies in different receptor families. For ADRB2 or ADRB1, the conformational change is initiated by contraction of the binding pocket due to the presence of hydrogen bonds between the agonist and residues in TM5, thus pulling TM5 closer to TM3 and TM6.[32,45,59] In addition to the inward movement of TM5, the twisting of the TM6 intracellular end

facilitates the interaction of the G_α subunit in the heterotrimeric G_s with the intracellular tip of TM5.

Figure 4 shows the hydrogen-bond occupancy computed along the multiple walker simulation trajectories of binary ADRB2 systems. Different occupancy patterns are observed from the hydrogen bond interactions, depending on the efficacy of the bound ligand. Some of these hydrogen-bond interactions are common to full agonists, partial agonists, and antagonists alike, while others are specific to full agonists only. In general, the most stable hydrogen-bond interactions are formed with residues $D^{3.32}$ and $N^{7.39}$, which are known to be anchor sites for the binding of most adrenergic ligands.[60]

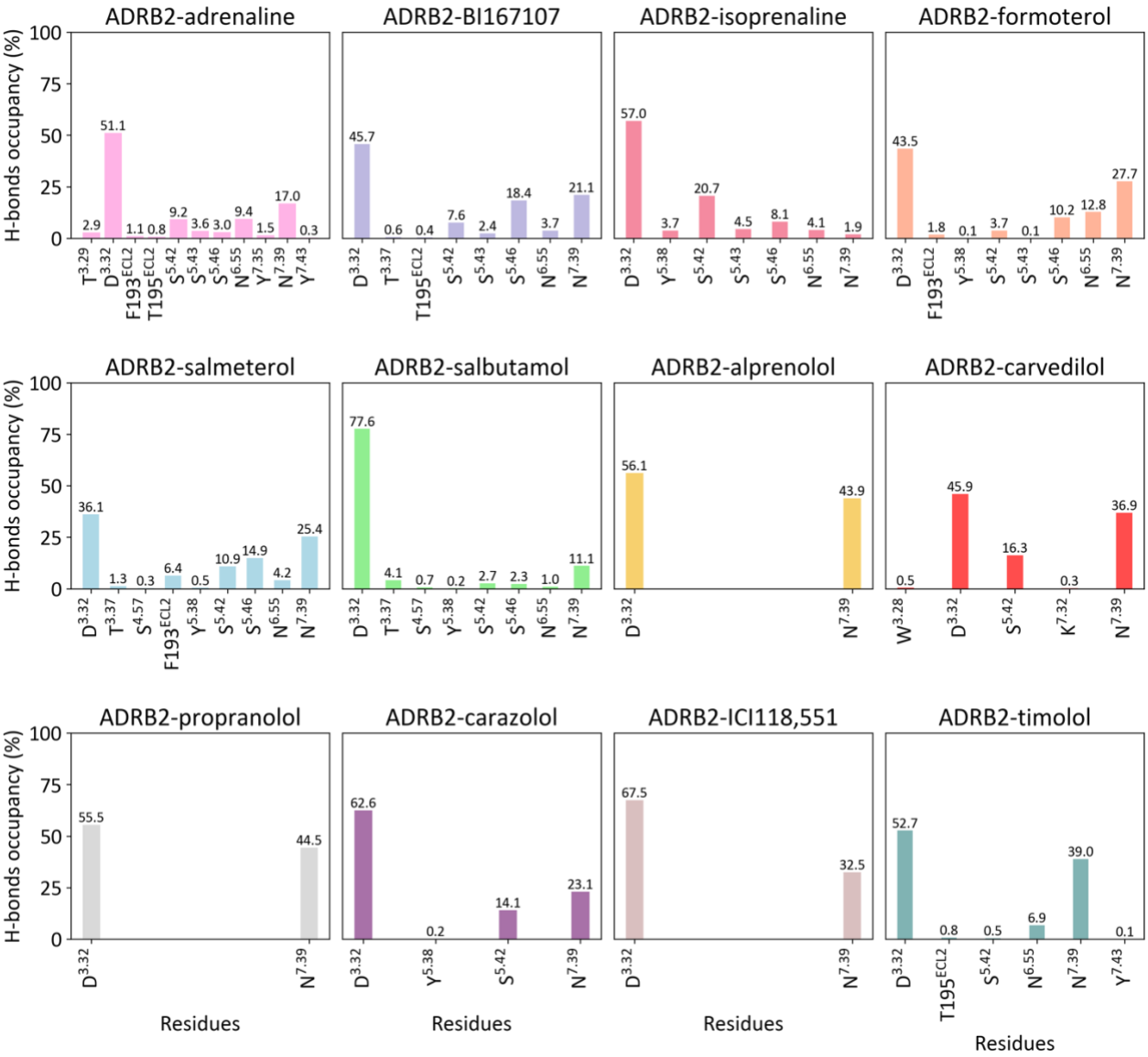

Figure 4. Hydrogen–bond occupancy sampled during the multiple walkers metadynamics simulations for ADRB2-ligand systems.

A complex hydrogen bond network between the catechol moiety and the serine residues $S^{5.42}$, $S^{5.43}$, and $S^{5.46}$ in TM5 is specific for full agonists (Figures 4 and 5), whereas it results partially formed in ADRB2 bound to partial agonists. These hydrogen bonds can be formed directly between the ligand and the receptor (Figure 5A, B and D) or can involve water-mediated polar interactions (Figure 5C). These polar interactions have been shown to stabilize a receptor conformation that includes an inward movement of the conserved $P^{5.50}$ and rearrangement of the residues associated

with the PIF motif in the receptor core.[6] As shown in Figure 5G, binary complexes with partial agonists resemble the inactive TM6 conformation observed in the carazolol-bound 2RH1 PDB structure, while a counterclockwise rotation relative to the inactive state can be observed for ADRB2 bound to full agonists. The inward movement of TM5 is incompatible with the packing arrangement of the PIF motif, so that a rotation of TM6 around $F^{6.44}$ is required in full agonist-ADRB2 binary complexes (Figure 5G, H).

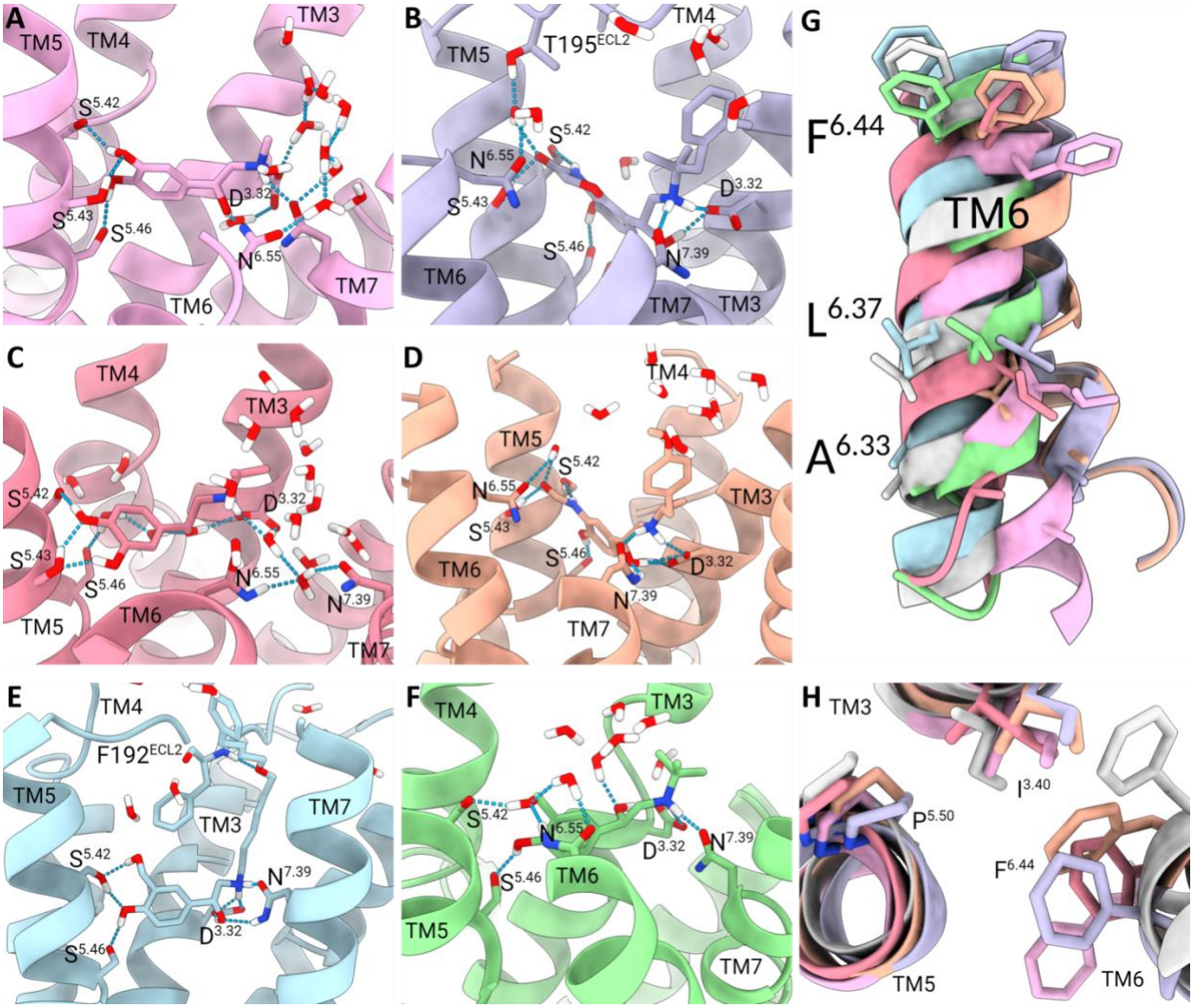

Figure 5. Comparison of agonists bound-ADRB2 binary complexes. (A-F) Polar interaction network formed in the binding pocket: (A) adrenaline (pink), (B) BI167107 (violet), (C) isoprenaline (light red), (D) formoterol (salmon), (E) salmeterol (cyan), (F) salbutamol (green). Water molecules with a cut-off distance lower than 0.5 nm are displayed (G) Representative view of theTM6 conformational rearrangement. (H) Representative view of the PIF Motif. Carazolol-bound 2RH1 PDB structure is represented in white.

Thus, we suggest that the polar interaction network observed in the serine-rich anchor site is responsible for the rotation and opening of the intracellular half of TM6 in binary complexes with full agonists. This would facilitate the binding of the $G_{\alpha s}$ subunit to form the final ternary complex, also providing a structural rationale for the higher energy barriers obtained for ADRB2 bound to partial agonists compared to full agonist binary complexes (Figures 1, and 2), because the former must overcome an additional energy barrier to rotate TM6.

Our results suggest that simultaneous polar interactions in TM5 anchor site are required to stabilize pre-active conformations in binary complexes with full agonists and play an essential role in ligand efficacy. Residues $S^{5.42}$, $S^{5.43}$, and $S^{5.46}$ have been shown to contribute to the affinity, potency, and efficacy of various catecholamine agonists.[9,14,61] Therefore, the subtle agonist-stabilized rearrangement in TM5 and TM6 promoted by the polar-interaction network in the serine-rich anchor site can initiate the cascade of structural changes involved in receptor activation and provide the molecular basis into the mechanism of action of partial agonist ligands.

CONCLUSIONS

The results shown above further support the applicability of our standard metadynamics protocol and the A^{100} activation index to study the activation process of class A GPCRs. We show that even if the conformational space of ADRB2 is sampled along a single CV the structural dynamics along key independent coordinates are not discarded. Indeed, through re-projection of the A^{100} free-energy profiles we were able to spot important structural features of the activation mechanism in presence of ligand with different efficacies and differentiate inactive structures of binary complexes with full and partial agonists.

All the results from the metadynamics simulations are consistent with the known pharmacology of the ligands studied here. Where the classification of ligands from the simulations is uncertain, this is also reflected in the experimental results. Ligand efficacy is mostly measured by a downstream biochemical (e.g., BRET and cAMP assays) or physiological response (e.g., smooth-muscle relaxation). Thus, measuring ligand efficacy is not trivial because the outcome of an agonist screen is closely linked to the environment of the cell and the sensitivity of the assay. For instance, formoterol has been classified either as a nearly full agonist or a partial agonist of high intrinsic efficacy.[62,63,64] In line with this observation are the similarity observed in the activation free-energy profiles between formoterol and salmeterol, and the structural differences observed in the microswitches considered here. Formoterol is the only full agonist in the series to shift the equilibrium for the microswitches towards more inactive-like conformations.

Several adrenergic ligands conventionally classified as antagonists have shown inverse agonism. Alprenolol is generally considered to be a neutral antagonist[35] but has also been observed to exhibit inverse-agonist properties.[65] Yao et al.[49] also suggest that alprenolol exhibits "*low partial-agonist activity*" and Wisler et al.[66] have pointed out that "*numerous classical neutral antagonists actually act as either partial agonists or inverse agonists*". Antagonists, such as carvedilol, and propranolol have also shown inverse agonist activity.[67] On the other hand, carvedilol, classed as an arrestin-biased ligand,[66] has been recently reported to exert its positive signaling through ADRB2 via low efficacy G-protein activation rather than arrestin-biased signaling.[17] Our results (Figure 2A) suggest that alprenolol and propranolol behave as neutral agonists, and a hint of agonistic activity is shown by carvedilol.

Importantly, the simulations have revealed a new and unexpected mode of action of partial agonists, ligands that can activate their receptor but to a lesser extent than full agonists.[68] Two

mechanisms for their mode of action have been proposed to explain ligand-dependent efficacy; partial agonists either stabilize a distinct ternary conformation that is less active than that stabilized by full agonists,[43,69] or they produce a lower concentration of the same active conformation as full agonists.[70] Our simulations suggest that the antagonist-like effect of both partial agonists salmeterol and salbutamol arises in the binary complex without the G-protein, rather than as alternative or intermediate conformations for the ternary complex. In this sense, we have shown the major role played by specific polar interactions with residues in TM5, which are required to stabilize an optimal TM6 conformation that facilitates G-protein binding and receptor activation. Combined with conformational sampling, our computed free energy landscapes provide energetics insights connecting ligand binding, to downstream conformational rearrangements required for receptor activation. In particular, our simulations have provided, on an atomistic level, direct evidence of structural requirements driving ligand efficacy and partial agonism at the β_2-adrenergic receptor. Thus, the results reported here constitute findings of remarkable value that contribute to the structure-based design of novel ligands with desired therapeutic efficacies.

COMPUTATIONAL METHODS

The details of the simulations and projection onto the microswitches, the entire activation/deactivation simulation protocol and the sources of the receptor structures used for initial equilibration are given in the Supporting Information.

ASSOCIATED CONTENT

Supporting Information. ADRB2 systems preparation protocol; microswitches definition; Histogram of the RMSD values of the global and secondary minima for the *apo*-ADRB2

metadynamics simulation; correlation plot between the mean A^{100}-value from MD runs and the deepest minimum identified in the A^{100} free-energy profiles; comparison of the activation free energy profiles obtained for three independent replicas of the ADRB2-isoprenaline system; results of the A^{100} MW-metadynamics simulation for three replicas of the ADRB2-isoprenaline system; A^{100} free-energy profiles reconstructed at increasing metadynamics sampling times; time evolution of the Gaussian hill height during the metadynamics simulations; comparison between the free energy as a function of the A^{100} calculated from the metadynamics bias potential and by reweighting for all ADRB2 systems; block analysis of the multiple-walkers metadynamics simulation for all ADRB2 systems; 2D free-energy landscapes projected onto the A^{100} index as function of: *i)* TM3-TM6 distance*, ii)* YY distance*, iii)* PIF RMSD, *iv)* NPxxY RMSD; time-series plots for: *i)* A^{100}, *ii)* TM3-TM6 distance, *iii)* YY distance, *iv)* PIF RMSD, *v)* NPxxY RMSD; dispersion plots showing A^{100} as a function of: *i)* TM3-TM6 distance, *ii)* YY distance, *iii)* PIF RMSD, *iv)* NPxxY RMSD; 2D free-energy landscapes projected onto the TM3-TM6 distance as function of: *i)* YY distance, *ii)* PIF RMSD, *iii)* NPxxY RMSD (PDF).

DATA AND SOFTWARE AVAILABILITY

All input files to run activation/deactivation MW-MetaD have been deposited to the public repository of the PLUMED consortium, PLUMED-NEST (plumID:23.016).

AUTHOR INFORMATION

Corresponding Authors

Timothy Clark − *Computer-Chemistry-Center, Department of Chemistry and Pharmacy, Friedrich-Alexander-University Erlangen-Nuernberg, 91052 Erlangen, Germany;* orcid.org/0000-0001-7931-4659; Email: Tim.Clark@fau.de

Francesco Luigi Gervasio − *Pharmaceutical Sciences, University of Geneva, CH1206 Geneva, Switzerland; Institute of Pharmaceutical Sciences of Western Switzerland, CH1206 Geneva, Switzerland; Chemistry Department, University College London, WC1H 0AJ London, U.K.*; orcid.org/0000-0003-4831-5039; Email: Francesco.Gervasio@unige.ch

Authors

Jacqueline C. Calderón − *Computer-Chemistry-Center, Department of Chemistry and Pharmacy, Friedrich-Alexander-University Erlangen-Nuernberg, 91052 Erlangen, Germany;* orcid.org/0000-0002-1505-0102

Passainte Ibrahim − *Institute of Medical Physics and Biophysics, Faculty of Medicine, University of Leipzig, 04107 Leipzig, Germany;* orcid.org/0000-0003-3208-7182

Dorothea Gobbo − *Pharmaceutical Sciences, University of Geneva, CH1206 Geneva, Switzerland; Institute of Pharmaceutical Sciences of Western Switzerland, CH1206 Geneva, Switzerland;* orcid.org/0000-0001-9102-710X

Author Contributions

The manuscript was written through contributions of all authors. All authors have given approval to the final version of the manuscript.

Funding Sources

Work in Erlangen was supported by the Deutsche Forschungsgemeinschaft as part of Research Training Group GRK 1910 “Medicinal Chemistry of Selective GPCR Ligands” and by grants of supercomputer time from the Gauss Alliance on SuperMUC (Project Nr. Pr74su) and from the Erlangen National High Performance Computing Center (NHR@FAU) of the Friedrich-Alexander-Universitaet Erlangen-Nuernberg (FAU). NHR funding was provided by federal and Bavarian state authorities. NHR@FAU hardware was partially funded by the DFG-Grant No. 440719683.

We acknowledge PRACE and the Swiss National Supercomputing Centre (CSCS) for large supercomputer time allocations on Piz Daint, project IDs: pr126, s1107. FLG acknowledges the Swiss National Science Foundation and Bridge for financial support (projects number: 200021_204795 and 40B2-0_203628).

Notes

The authors declare no competing financial interest.

ABBREVIATIONS

ADRB2, β_2-adrenergic receptor; ADRB1, β_1-adrenergic receptor; MD, molecular dynamics; PDB, Protein Data Bank; RMSD, root mean squared deviation; 1D, one-dimensional; 2D, two-dimensional; CV, collective variable.

REFERENCES

1 Bjarnadóttir, T. K.; Gloriam, D. E.; Hellstrand, S. H.; Kristiansson, H.; Fredriksson, R.; Schiöth, H. B. Comprehensive repertoire and phylogenetic analysis of the G protein-coupled receptors in human and mouse. *Genomics* **2006**, *88*, 263–273.

2 Dror, R. O.; Arlow, D. H.; Maragakis, P.; Mildorf, T. J.; Pan, A. C.; Xu, H.; Borhani, D. W.; Shaw, D. E. Activation mechanism of the β_2-adrenergic receptor. *Proc. Natl. Acad. Sci. U.S.A.* **2011**, *108*, 18684–18689.

3 Kohlhoff, K. J.; Shukla, D.; Lawrenz, M.; Bowman, G. R.; Konerding, D. E.; Belov, D.; Altman, R. B.; Pande, V. S. Cloud-based simulations on Google Exacycle reveal ligand modulation of GPCR activation pathways. *Nature Chem.* **2014**, *6*, 15–21.

4 Fleetwood, O.; Matricon, P.; Carlsson, J.; Delemotte, L. Energy landscapes reveal agonist control of G protein-coupled receptor activation via microswitches. *Biochem*. **2020**, *59*, 880−891.

5 Fleetwood, O.; Carlsson, J.; Delemotte, L. Identification of ligand-specific G protein-coupled receptor states and prediction of downstream efficacy via data-driven modeling. *eLife* **2021**, *10*, e60715.

6 Rasmussen, S. G. F.; Choi, H.-J.; Fung, J. J.; Pardon, E.; Casarosa, P.; Chae, P. S.; DeVree, B. T.; Rosenbaum, D. M.; Thian, F. S.; Kobilka, T. S.; Schnapp, A.; Konetzki, I.; Sunahara, R. K.; Gellman, S. H.; Pautsch, A.; Steyaert, J.; Weis, W. I.; Kobilka, B. K. Structure of a nanobody-stabilized active state of the β_2 adrenoceptor. *Nature* **2011***, 469*, 175–180.

7 Rasmussen, S. G. F.; DeVree, B. T.; Zou, Y.; Kruse, A. C.; Chung, K. Y.; Kobilka, T. S.; Thian, F. S.; Chae, P. S.; Pardon, E.; Calinski, D.; Mathiesen, J. M.; Shah, S. T. A.; Lyons, J. A.; Caffrey, M.; Gellman, S. H.; Steyaert, J.; Skiniotis, G.; Weis, W. I.; Sunahara, R. K.; Kobilka, B. K. Crystal structure of the β_2 adrenergic receptor–Gs protein complex. *Nature* **2011**, *477*, 549–555.

8 Liu, J. J.; Horst, R.; Katritch, V.; Stevens, R. C.; Wuthrich, K. Biased signaling pathways in β_2-adrenergic receptor characterized by ^{19}F-NMR. *Science* **2012,** *335*, 1106–1110.

9 Masureel, M.; Zou, Y.; Picard, L.-P.; van der Westhuizen, E.; Mahoney, J. P.; Rodrigues, J. P. G. L. M.; Mildorf, T. J.; Dror, R. O.; Shaw, D. E.; Bouvier, M.; Pardon, E.; Steyaert, J.; Sunahara,

R. K.; Weis, W. I.; Zhang, C.; Kobilka, B. K. Structural insights into binding specificity, efficacy and bias of a β2AR partial agonist. *Nat. Chem. Biol.* **2018**, *14*, 1059−1066.

10 Liu, X.; Kaindl, J.; Korczynska, M.; Stößel, A.; Dengler, D.; Stanek, M.; Hübner, H.; Clark, M. J.; Mahoney, J.; Matt, R. A.; Xu, X.; Hirata, K.; Shoichet, B. K.; Sunahara, R. K.; Kobilka, B. K.; Gmeiner, P. An allosteric modulator binds to a conformational hub in the β_2 adrenergic receptor. *Nature Chem. Biol.* **2020***, 16*, 749–755.

11 Dror, R. O.; Arlow, D. H.; Borhani, D. W.; Jensen, M. Ø.; Piana, S.; Shaw, D. E. Identification of two distinct inactive conformations of the β_2-adrenergic receptor reconciles structural and biochemical observations. *Proc. Natl. Acad. Sci. U.S.A.* **2009**, *106*, 4689–4694.

12 Tikhonova, I. G.; Selvam, B.; Ivetac, A.; Wereszczynski, J.; McCammon, J. A. Simulations of biased agonists in the β_2 adrenergic receptor with accelerated molecular dynamics. *Biochem.* **2013**, *52*, 5593–5603.

13 van der Westhuizen, E. T.; Breton, B.; Christopoulos, A.; Bouvier, M. Quantification of ligand bias for clinically relevant β_2-adrenergic receptor ligands: implications for drug taxonomy. *Mol. Pharmacol.* **2014***, 85*, 492–509.

14 Katritch, V.; Reynolds, K. A.; Cherezov, V.; Hanson, M. A.; Roth, C. B.; Yeager, M.; Abagyan, R. Analysis of full and partial agonists binding to β_2-adrenergic receptor suggests a role of transmembrane helix V in agonist-specific conformational changes. *J. Mol. Recognit.* **2009**, *22*, 307–318.

15 Grahl, A.; Abiko, L. A.; Isogai, S.; Sharoe, T.; Grzesiek, S. A high-resolution description of β_1-adrenergic receptor functional dynamics and allosteric coupling from backbone NMR. *Nature Commun.* **2020**, *11*, 2216.

16 Imai, S.; Yokomizo, T.; Kofuku, Y.; Shiraishi, Y.; Ueda, T.; Shimada, I. Structural equilibrium underlying ligand dependent activation of β_2-adrenoreceptor. *Nat. Chem. Biol.* **2020**, *16*, 430–439.

17 Benkel, T.; Zimmermann, M.; Zeiner, J.; Bravo, S.; Merten, V.; Lim, V. J. Y.; Matthees, E. S. F.; Drube, J.; Miess-Tanneberg, E.; Malan, D.; Szpakowska, M.; Monteleone, S.; Grimes, J.; Koszegi, Z.; Lanoiselée, Y.; O'Brien, S.; Pavlaki, N.; Dobberstein, N.; Inoue, A.; Nikolaev, V.; Calebiro, D.; Chevigné, A.; Sasse, P.; Schulz, S.; Hoffmann, C.; Kolb, P.; Waldhoer, M.; Simon,

K.; Gomeza, J.; Kostenis, E. How carvedilol activates β_2-adrenoceptors. *Nature Commun*. **2022**, *13*, 7109.

18 Baker, J. G. The selectivity of β -adrenoceptor antagonists at the human β_1, β_2 and β_3 adrenoceptors. *Br. J. Pharmacol.* **2005**, *144*, 317–322.

19 Wu, Y.; Zeng, L.; Zhao, S. Ligands of adrenergic receptors: a structural point of view. *Biomolecules* **2021**, *11*, 936.

20 Zhu, B. T. Rational design of receptor partial agonists and possible mechanisms of receptor partial activation: a theory. *J. Theor. Biol.* **1996***, 181*, 273–291.

21 Nygaard, R.; Zou, Y.; Dror, R. O.; Mildorf, T. J.; Arlow, D. H.; Manglik, A.; Pan, A. C.; Liu, C. W.; Fung, J. J.; Bokoch, M. P.; Thian, F. S.; Kobilka, T. S.; Shaw, D. E.; Mueller, L.; Prosser, R. S.; Kobilka, B. K. The dynamic process of β_2-adrenergic receptor activation. *Cell* **2013**, *152*, 532–542.

22 Bhattachary, S.; Vaidehi, N. Computational mapping of the conformational transitions in agonist selective pathways of a G-protein coupled receptor. *J. Am. Chem. Soc.* **2010**, *132*, 5205–5214.

23 Hu, X.; Wang, Y.; Hunkele, A.; Provasi, D.; Pasternak, G. W.; Filizola, M. Kinetic and thermodynamic insights into sodium ion translocation through the μ-opioid receptor from molecular dynamics and machine learning analysis. *PLOS Comput. Biol.* **2019**, *15*, e1006689.

24 Li, J.; Jonsson, A. L.; Beuming, T.; Shelley, J. C.; Voth, G. A. Ligand-dependent activation and deactivation of the human adenosine A_{2A} receptor. *J. Am. Chem. Soc.* **2013**, *135*, 8749–8759.

25 Miao, Y.; McCammon, J. A. Graded activation and free energy landscapes of a muscarinic G-protein-coupled receptor. *Proc. Natl. Acad. Sci. U.S.A.* **2016**, *113*, 12162–12167.

26 Alhadeff, R.; Vorobyov, I.; Yoon, H. W.; Warshel, A. Exploring the free-energy landscape of GPCR activation. *Proc. Natl. Acad. Sci. U.S.A.* **2018**, *115*, 10327–10332.

27 Mondal, D.; Kolev, V.; Warshel, A. Exploring the activation pathway and Gi-coupling specificity of the μ-opioid receptor. *Proc. Natl. Acad. Sci. U.S.A.* **2020**, *117*, 26218–26225.

28 Yang, Y. I.; Shao, Q.; Zhang, J.; Yang, L.; Gao, Y. Q. Enhanced sampling in molecular dynamics. *J. Chem. Phys.* **2019**, *151*, 070902.

29 Mattedi, G.; Acosta-Gutiérrez, S.; Clark, T.; Gervasio, F. L. A combined activation mechanism for the glucagon receptor. *Proc. Nat. Acad. Sci. U.S.A.* **2020**, *117*, 15414–15422.

30 Saleh, N.; Ibrahim, P.; Saladino, G.; Gervasio, F. L.; Clark, T. An efficient metadynamics-based protocol to model the binding affinity and the transition state ensemble of G-protein-coupled receptor ligands. *J. Chem. Inf. Model.* **2017**, *57*, 1210–1217.

31 Calderón, J. C.; Ibrahim, P.; Gobbo, D.; Gervasio, F. L.; Clark. T. A general metadynamics protocol to simulate activation/deactivation of class A GPCRs: proof of principle for the serotonin receptor. *J. Chem. Inf. Model.* **2023**, *63*, 3105–3117.

32 Ring, A. M.; Manglik, A.; Kruse, A. C.; Enos, M. D.; Weis, W. I.; Garcia, K. C.; Kobilka, B. K. Adrenaline-activated structure of β_2-adrenoceptor stabilized by an engineered nanobody. *Nature* **2013**, *502*, 575–579.

33 Yang, F.; Ling, S.; Zhou, Y.; Zhang, Y.; Lv, P.; Liu, S.; Fang, W.; Sun, W.; Hu, L. A.; Zhang, L.; Shi, P.; Tian, C. Different conformational responses of the β_2-adrenergic receptor-Gs complex upon binding of the partial agonist salbutamol or the full agonist isoprenaline. *Natl. Sci. Rev*. **2021**, *8*, nwaa284.

34 Zhang, Y.; Yang, F.; Ling, S.; Lv, P.; Zhou, Y.; Fang, W.; Sun, W.; Zhang, L.; Shi, P.; Tian, C. Single-particle cryo-EM structural studies of the β_2AR–Gs complex bound with a full agonist formoterol. *Cell Discov.* **2020**, *6*, 45.

35 Wacker, D.; Fenalti, G.; Brown, M. A.; Katritch, V.; Abagyan, R.; Cherezov, V.; Stevens, R. C. Conserved binding mode of human β_2 adrenergic receptor inverse agonists and antagonist revealed by X-ray crystallography. *J. Am. Chem. Soc.* **2010**, *132*, 11443–11445.

36 Ishchenko, A.; Stauch, B.; Han, G. W.; Batyuk, A.; Shiriaeva, A.; Li, C.; Zatsepin, N.; Weierstall, U.; Liu, W.; Nango, E.; Nakane, T.; Tanaka, R.; Tono, K.; Joti, Y.; Iwata, S.; Moraes, I.; Gati, C.; Cherezov, V. Toward G protein-coupled receptor structure-based drug design using X-ray lasers. *IUCrJ* **2019**, *6*, 1106–1119.

37 Cherezov, V.; Rosenbaum, D. M.; Hanson, M. A.; Rasmussen, S. G. F.; Thian, F. S.; Kobilka, T. S.; Choi, H.-J.; Kuhn, P.; Weis, W. I.; Kobilka, B. K.; Stevens, R. C. High-resolution crystal structure of an engineered human β_2-adrenergic G protein-coupled receptor. *Science* **2007**, *318*, 1258–1265.

38 Nygaard, R.; Frimurer, T. M.; Holst, B.; Rosenkilde, M. M.; Schwartz, T. W. Ligand binding and micro-switches in 7TM receptor structures. *Trends Pharmacol. Sci*. **2009**, *30*, 249–259.

39 Solt, A. S.; Bostock, M. J.; Shrestha, B.; Kumar, P.; Warne, T.; Tate, C. G.; Nietlispach, D. Insight into partial agonism by observing multiple equilibria for ligand-bound and Gs-mimetic nanobody-bound β_1-adrenergic receptor. *Nature Commun*. **2017**, *8*, 1795.

40 Ibrahim, P.; Wifling, D.; Clark, T. A universal activation index for class A GPCRs. *J. Chem. Inf. Model.* **2019**, *59*, 3938–3945.

41 Raiteri, P.; Laio, A.; Gervasio, F. L.; Micheletti, C.; Parrinello, M. Efficient reconstruction of complex free energy landscapes by multiple walkers metadynamics. *J. Phys. Chem. B* **2006**, *110*, 3533–3539.

42 Dama, D. F.; Parrinello, M.; Voth, G. A. Well-tempered metadynamics converges asymptotically. *Phys. Rev. Lett.* **2014**, *112*, 240602.

43 Kobilka, B. K.; Deupi, X. Conformational complexity of G-protein-coupled receptors. *Trends. Pharmacol. Sci.* **2007**, *28*, 397–406.

44 Manglik, A.; Kim, T. H.; Masureel, M.; Altenbach, C.; Yang, Z.; Hilger, D.; Lerch, M. T.; Kobilka, T. S.; Thian, F. S.; Hubbell, W. L.; Prosser, R. S.; Kobilka, B. K. Structural insights into the dynamic process of β_2-adrenergic receptor signaling. *Cell* **2015**, *161*, 1101–1111.

45 Weis, W. I.; Kobilka, B. K. The molecular basis of G protein–coupled receptor activation. *Ann. Rev. Biochem.* **2018**, *87*, 897–919.

46 Seifert, R.; Wenzel-Seifert, K. Constitutive activity of G-protein-coupled receptors: cause of disease and common property of wild-type receptors. *Naunyn-Schmiedeberg's Arch. Pharmacol.* **2002**, *366*, 381–416.

47 Lamichhane, R.; Liu, J. J.; Pljevaljcic, G.; White, K. L.; van der Schans, E.; Katritch, V.; Stevens, R. C.; Wüthrich, K.; Millar, D. P. Single-molecule view of basal activity and activation mechanisms of the G protein-coupled receptor β_2AR. *Proc. Nat. Acad. Sci. U.S.A.* **2015**, *112*, 14254–14259.

48 Saleh, M.; Saladino, G.; Gervasio, F. L.; Clark, T. Investigating allosteric effects on the functional dynamics of β2-adrenergic ternary complexes with enhanced-sampling simulations. *Chem. Sci.*, **2017**, *8*, 4019-4026.

49 Yao, X. J.; Vélez Ruiz, G.; Whorton, M. R.; Rasmussen, S. G. F.; DeVree, B. T.; Deupi, X.; Sunahara, R. K.; Kobilka, B. The effect of ligand efficacy on the formation and stability of a GPCR-G protein complex. *Proc. Nat. Acad. Sci. U.S.A.* **2009**, *106*, 9501–9506.

50 Ghanouni, P.; Gryczynski, Z.; Steenhuis, J. J.; Lee, T. W.; Farrens, D. L.; Lakowicz, J. R.; Kobilka, B. K. Functionally different agonists induce distinct conformations in the G-protein coupling domain of the β_2 adrenergic receptor. *J. Biol. Chem.* **2001**, *276*, 24433–24436.

51 Elster, L.; Elling, C.; Heding, A. Bioluminescence resonance energy transfer as a screening assay: focus on partial and inverse agonism. *J. Biomol. Screen.* **2007**, *12*, 41–49.

52 Lemoine, H.; Overlack, C.; Köhl, A.; Worth, H.; Reinhardt, D. Formoterol, fenoterol, and salbutamol as partial agonists for relaxation of maximally contracted guinea pig tracheae: comparison of relaxation with receptor binding. *Lung* **1992**, *170*, 163–180.

53 Moore, R. H.; Khan, A.; Dickey, B. F. Long-acting inhaled β_2-agonists in asthma therapy. *CHEST* **1998**, *113*,1095–1108.

54 Rosenbaum, D. M.; Zhang, C.; Lyons, J. A.; Holl, R.; Aragao, D.; Arlow, D. H.; Rasmussen, S. G. F.; Choi, H.-J.; DeVree, B. T.; Sunahara, R. K.; Chae, P. S.; Gellman, S. H.; Dror, R. O.; Shaw, D. E.; Weis, W. I.; Caffrey, M.; Gmeiner, P.; Kobilka, B. K. Structure and function of an irreversible agonist-β_2 adrenoceptor complex. *Nature* **2011**, *469*, 236–240.

55 Warne, T.; Moukhametzianov, R.; Baker, J. G.; Nehmé, R.; Edwards, P. C.; Leslie, A. G. W.; Schertler, G. F. X.; Tate, C. G. The structural basis for agonist and partial agonist action on a β_1-adrenergic receptor. *Nature* **2011**, *469*, 241–244.

56 Qu, L.; Zhou, Q. T.; Wu, D.; Zhao, S. W. Crystal structure of the alpha2A adrenergic receptor in complex with a partial agonist. PDB Entry - 6KUY. Available at https://doi.org/10.2210/pdb6kuy/pdb

57 Bock, A.; Bermudez, M. Allosteric coupling and biased agonism in G-Protein-coupled receptors. *FEBS* **2021**, *288*, 2513–2528.

58 Eddy, M. T.; Martin, B. T.; Wüthrich, K. A_{2A} adenosine receptor partial agonism related to structural rearrangements in an activation microswitch. *Structure* **2021**, *29*, 170–176.

59 Kobilka, B. The structural basis of G-protein-coupled receptor signaling (Nobel lecture). *Angew. Chem. Int. Ed.* **2013**, *52*, 6380–6388.

60 Strader, C. D.; Sigal, I. S.; Candelore, M. R.; Rands, E.; Hill, W. S.; Dixon, R. A. Conserved aspartic acid residues 79 and 113 of the beta-adrenergic receptor have different roles in receptor function. *J. Biol. Chem.* **1988**, *263*, 10267–10271.

61 Strader, C. D.; Candelore, M. R.; Hill, W. S.; Sigal, I. S.; Dixon, R. A. Identification of two serine residues involved in agonist activation of the β-adrenergic receptor. *J. Biol. Chem*. **1989**, *264*, 13572–13578.

62 Naline, E.; Trifilieff, A.; Fairhurst, R. A.; Advenier, C.; Molimard, M. Effect of indacaterol, a novel long-acting β_2-agonist, on isolated human bronchi. *Eur. Respir. J.* **2007**, *29*, 575–581.

63 O'Byrne, P. M.; Satia, I. Inhaled β_2-agonist. In *Middleton's Allergy Principles and Practice*, 9th ed.; Burks, A. W.; Holgate, S. T.; O'Hehir, R. E.; Broide, D. H.; Bacharier, L. B.; Hershey, G. K. K.; Peebles, R. S.; Eds.; Elsevier Inc, 2020; pp 1518–1524.

64 Kume, H. Clinical use of β_2-adrenergic receptor agonists based on their intrinsic efficacy. *Allergol. Int.* **2005**, *54*, 89–97.

65 Varma, D. R.; Shen, H.; Deng, X. F.; Peri, K. G.; Chemtob, S.; Mulay, S. Inverse agonist activities of β-adrenoceptor antagonists in rat myocardium. *Br. J. Pharmacol.* **1999**, *127*, 895–902.

66 Wisler, J. W.; DeWire, S. M.; Whalen, E. J.; Violin, J. D.; Drake, M. T.; Ahn, S.; Shenoy, S. K.; Lefkowitz, R. J. A unique mechanism of β-blocker action: Carvedilol stimulates β-arrestin signaling. *Proc. Natl. Acad. Sci. U.S.A.* **2007**, *104*, 16657–16662.

67 Nagaraja, S.; Iyer, S.; Liu, X.; Eichberg, J.; Bond, R. A. Treatment with inverse agonists enhances baseline atrial contractility in transgenic mice with chronic beta2-adrenoceptor activation. *Br. J Pharmacol.* **1999**, *127*, 1099–1104.

68 Clark, R. B.; Knoll, B. J.; Barber, R. Partial agonists and G protein-coupled receptor desensitization. *Trends Pharmacol. Sci.* **1999**, *20*, 279–286.

69 Seifert, R.; Wenzel-Seifert, K.; Gether, U.; Kobilka, B. K. Functional differences between full and partial agonists: Evidence for ligand-specific receptor conformations. *J. Pharmacol. Exp. Ther.* **2001**, *297*,1218–1226.

70 Nikolaev, V. O.; Hoffmann, C.; Bünemann, M.; Lohse, M. J.; Vilardaga, J.-P. Molecular basis of partial agonism at the neurotransmitter α_{2A}-adrenergic receptor and Gi-protein heterotrimer. *J. Biol. Chem.* **2006**, *281*, 24506–24511.

ToC Graphic

Activation/Deactivation Free-Energy Profiles for the β_2-Adrenergic Receptor: Ligand Modes of Action Jacqueline C. Calderón, Passainte Ibrahim, Dorothea Gobbo, Francesco Luigi Gervasio and Timothy Clark